Rayleigh-Type Wave in A Rotated Piezoelectric Crystal Imperfectly Bonded on a Dielectric Substrate

Guoquan Nie[1, *] and Menghe Wang[1]

Abstract: Propagation characteristics of Rayleigh-type wave in a piezoelectric layered system are theoretically investigated. The piezoelectric layer is considered as a cubic crystal with finite thickness rotated about *Y*-axis and is imperfectly bonded onto a semi-infinite dielectric substrate. The imperfect interface between the two constituents is assumed to be mechanically compliant and dielectrically weakly conducting. The exact dispersion relations for electrically open or shorted boundary conditions are obtained. The numerical results show that the phase velocity of Rayleigh-type wave is symmetric with respect to the cut orientation of $45°$ and can achieve the maximum propagation speed in this orientation. The mechanical imperfection plays an important role in the dispersion relations, further the normal imperfection can produce a significant reduction of phase velocity comparing with the tangential imperfection. Comparing with the mechanical imperfection the electrical imperfection makes a relatively small reduction of phase velocity of Rayleigh-type wave. The obtained results can provide some fundamentals for understanding of piezoelectric semiconductor and for design and application of piezoelectric surface acoustic wave devices.

Keywords: Piezoelectric cubic crystal, Rayleigh-type wave, imperfect interface, cut orientation, dispersion relation.

1 Introduction

Due to being able to achieve the conversion between mechanical energy and electrical energy, surface acoustic wave (SAW) devices made of piezoelectric materials are widely used as resonators, tunable filters, delay lines, sensing devices, energy harvesters and micro-electro-mechanical systems [Jakoby and Vellekoop (1997); Garner and Ohkawa (2002); Campbell and Jones (1968); Ma and Wu (2009); Ghasemi, Park and Rabczuk (2017); Ghasemi, Park and Rabczuk (2018); Hamdia, Ghasemi, Zhuang et al. (2018); Nanthakumar, Lahmer, Zhuang et al. (2016); Nanthakumar, Zhuang, Park et al. (2017); Nguyen, Nanthakumar, Zhuang et al. (2018); Thai, Rabczuk and Zhuang (2018)]. Studies of wave propagation in piezoelectric media and structures have been the subject of increasing research activity for about 50 years. At the earliest, Bluestein [Bluestein (1968)] and Gulyaev [Gulyaev (1968)] almost concurrently discovered that a shear horizontal (SH) surface wave can propagate in the hexagonal 6mm piezoelectric

---

[1] Department of Engineering Mechanics, Shijiazhuang Tiedao University, Shijiazhuang, 050043, China.

[*] Corresponding Author: Guoquan Nie. Email: niegq@stdu.edu.cn.

half-space when its surface is electrically shorted or open to the vacuum, and thus be commonly termed as Bleustein-Gulyaev (BG) wave. BG wave is a non-dispersive surface wave which exists only in piezoelectric materials. Like the Love wave its particle motion is entirely transverse and parallel to the surface, but it is confined to the surface by the piezoelectric effect rather than by a layer of a different material. These characteristics of non-dispersive and large penetration depth of BG wave greatly restricts its practical applications in acoustic and microwave devices. But if the piezoelectric half-space is replaced by a layered structure, such disadvantages of BG wave can be dramatically alleviated [Curtis and Redwood (1973); Sun and Cheng (1974)]. Many efforts therefore have been made to explore the propagation of surface waves in piezoelectric layered structures in recent decades. According to the material properties and stacking sequence of the covering layer and the substrate, piezoelectric layered systems can be classified into three forms, i.e., elastic layer/piezoelectric substrate [Curtis and Redwood (1973); Zhang and Feng (2012)], piezoelectric layer/elastic substrate [Qian, Jin and Hirose (2011); Qian and Hirose (2012); Nie, Liu and Li (2015); Singh, Parween, Kumar et al. (2018); Singh, Das, Mistri et al. (2017)], and piezoelectric layer/piezoelectric substrate [Morocha (2010); Zakharenko (2005); Singh, Kumar and Chattopadhyay (2015)]. Most of the published results on piezoelectric surface waves are for polarized ceramics and quartz for transducer and acoustic wave resonator or sensor. One of the most common types of piezoelectric crystals is the cubic crystal system which possesses the same form of macroscopic symmetry to the piezoelectric semiconductor. So, study on wave propagation in cubic crystals can offer some fundamentals for the understanding and application of piezoelectric semiconductor, such as acoustic wave amplification, stress and strain sensing, energy harvesting and conversion [Chen, Wang, Du et al. (2016)]. Many researchers focused on the various wave propagating in piezoelectric cubic crystals. Tseng [Tseng (1970)] demonstrated that the elastic Rayleigh waves and the SH-PE surface wave can propagate in piezoelectric cubic crystals of $\overline{4}3m$ and 23 classes along the [110] direction on the $(\overline{1}10)$ surface and their equivalent orientation, and the velocity equations for the piezoelectric surface wave and elastic surface wave were derived. Bright and Hunt [Bright and Hunt (1989)] explored an analytical solution for BG piezoelectric surface wave in cubic crystals. A general formulation of the boundary-value problem and the equation of power carried by the BG wave were presented. The existence of BG wave in six kinds of piezoelectric cubic crystals was demonstrated in their numerical examples. Rio et al. [Rio and Velasco (1985)] studied the surface wave propagating on the (100) and (110) surfaces of piezoelectric cubic crystal by using the surface Green function matching method. They found that there is no BG wave can propagate along the [100] and [110] symmetry directions on the (100) surface, while on the (110) surface BG wave can propagate along the $[1\overline{1}0]$ symmetry direction and a piezoelectric Rayleigh wave along the $[00\overline{1}]$ direction. Zakharenko [Zakharenko (2005)] investigated the propagation of Love wave in layered half-space systems consisting of two class-23 cubic piezoelectric media, and the dispersion relations for seven partial Love-type waves were obtained numerically. Zakharenko [Zakharenko (2010)] gave a further study on interfacial SH wave propagating along the interface of

two piezoelectric cubic crystals of $\overline{4}3m$ and 23 classes. It was found that this kind of interfacial SH wave can always propagate along the interface of two identical piezoelectric crystals with opposite polarization.

In the studies mentioned above, the interface existing in layered system or bi-material space was considered as a perfect bonding. It is well known that the interfacial imperfection can weaken the stiffness and continuity of layered system, and further affects the wave propagation behaviors [Nie, Liu and Liu (2016)]. Considering interface imperfection, many efforts have been made on the propagation of surface waves [Liu, Wang and Wang (2010); Fan, Yang and Xu (2006); Li and Jin (2012); Singh, Chaki, Hazra et al. (2017); Singh, Kumar and Kumari (2018)] and interfacial waves [Chen, Hu and Yang (2008); Xu, Fan, Chen et al. (2006); Fan, Yang and Xu (2006); Huang and Li (2011)] in various layered structures or bi-material systems with a constituent of piezoelectric media. However, the interfacial imperfection mentioned was restricted to pure mechanical imperfection while the electrical imperfection was not considered. In fact, defects and damages to the interface are often inevitable due to electro-mechanical coupling and fatigue. Therefore, the effects of both mechanical and electrical imperfection are interesting for piezoelectric devices. Recently, Li et al. [Li, Wei and Guo (2016)] studied the propagation of Rayleigh wave in a system consisting of an elastic half-space carrying a piezoelectric gradient covering layer. Five types of gradient profiles and two types of imperfect interfaces were considered and the effects of the mechanical and dielectric interface parameters on surface wave speed are discussed. Similarly, Li et al. [Li and Lee (2010)] investigated SH wave propagating in a cylindrical piezoelectric sensor with both mechanically and electrically interfacial imperfection.

This work is firstly motivated by the growing interest in piezoelectric semiconductors which are common cubic crystals. For the design and application of piezoelectric semiconductor devices, knowledge of the electric field accompanying mechanical deformation or acoustic waves from a piezoelectric analysis is fundamental. However, available theoretical results for cubic crystals are limited and most of them are for anti-plane problems. Rayleigh waves, however, are free plane waves propagating along the surface of a semi-infinite solid which were first theoretically predicted in 1885. While the traction forces must vanish on the boundary and the energy must decay with increased depth. Since the middle of the 20th century, Rayleigh waves were widely employed in a number of areas of science and technology, including ultrasonic nondestructive testing, structural health monitoring, electronic circuitry and other surface acoustic waves devices [Lewis (1995)]. On the other hand, the interface of layered system consisting of two types of materials is always imperfect bonding in most practical case due to various causes such as the microdefect and porosity processed in solid-state sintering, the aging of the glue, the corrosion of constituent materials, the accumulated damage or the local debond under harsh working circumstances, and so on [Lavrentyev and Rokhlin (1998); Vig and Ballato (1998)]. The imperfect bonding can greatly affect the performances of layered composites or devices. In this paper, we study the Rayleigh-type wave propagating in piezoelectric layered systems of cubic crystal. A declination angle between the direction of Rayleigh-type wave propagation and the crystallographic axis is considered. Effects of the mechanical and electrical interface parameters on dispersion curve and phase velocity

are discussed based on the numerical results.

2 Problem formulations and basic equations

Consider a piezoelectric layered structure as shown in Fig. 1. The covering layer is a piezoelectric cubic crystal with finite thickness h and imperfectly bonding onto an isotropic dielectric substrate. Let the *XYZ* coordinate system aligns with the crystallographic axes of piezoelectric cubic crystal. Cut the piezoelectric crystal along a plane containing the *Y*-axis and rotating an angle θ with the *XY* plane so that a new rectangular Cartesian coordinate system $x_1x_2x_3$ can be obtained. We suppose that Rayleigh wave propagate along the x_1-axis in the x_1x_3 plane and hence a plane strain state can be produced. For convenience, the rotated coordinate system $x_1x_2x_3$ is adopted in the following analysis.
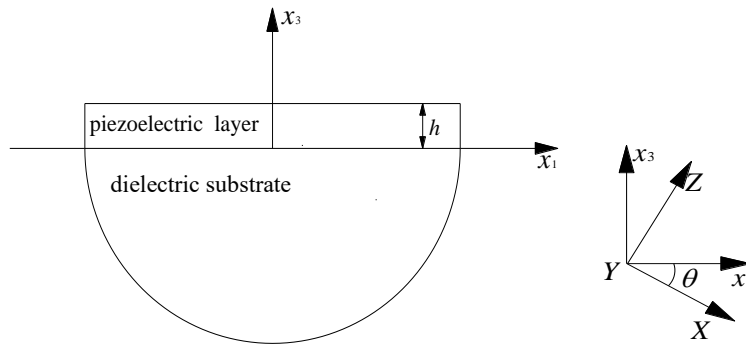

Figure 1: Geometry of a rotated piezoelectric layered system

According to the plane strain assumption, all field variables are independent on coordinate x_2 and the mechanical displacement components can be reduced to two-dimensional case with $u_1=u_1(x_1,x_3,t)$ and $u_3=u_3(x_1,x_3,t)$. The electric potential is $\varphi=\varphi(x_1,x_3,t)$. According to the quasi-static approximation, in the absence of body forces and free charges, the equations of motion and the electric field equations in the sagittal plane are given by

$$\frac{\partial \sigma_{11}}{\partial x_1}+\frac{\partial \sigma_{13}}{\partial x_3}=\rho \ddot{u}_1$$

$$\frac{\partial \sigma_{13}}{\partial x_1}+\frac{\partial \sigma_{33}}{\partial x_3}=\rho \ddot{u}_3 \tag{1}$$

$$\frac{\partial D_1}{\partial x_1}+\frac{\partial D_3}{\partial x_3}=0$$

where σ_{11}, σ_{13} and σ_{33} are the stress components, D_1 and D_3 are the electric displacements, ρ is the mass density. A superimposed dot represents the differentiation with respect to time t. Once u_1, u_3 and φ are determined from appropriate conditions, the nonzero stresses σ_{11}, σ_{13} and σ_{33} as well as the electric displacements D_1 and D_3 can be given through the

following constitutive relations [Tseng (1970)]:

$$\sigma_{11} = c_{11}u_{1,1} + c_{13}u_{3,3} + e_{31}\varphi_{,3}$$

$$\sigma_{33} = c_{13}u_{1,1} + c_{33}u_{3,3}$$

$$\sigma_{13} = c_{44}\left(u_{1,3} + u_{3,1}\right) + e_{15}\varphi_{,1} \tag{2}$$

$$D_1 = e_{15}\left(u_{1,3} + u_{3,1}\right) - \varepsilon_{11}\varphi_{,1}$$

$$D_3 = e_{31}u_{1,1} - \varepsilon_{11}\varphi_{,3}$$

where c_{11}, c_{13}, c_{33} and c_{44} are elastic constants, e_{31} and e_{15} are the piezoelectric constants, ε_{11} is the dielectric constant. The above material constants are related to the corresponding quantities c'_{11}, c'_{12}, c'_{44}, e'_{14}, ε'_{11} in the crystallographic coordinate system *XYZ* and can be obtained through tensor transformations as

$$c_{11} = \left(\cos^4\theta + \sin^4\theta\right)c'_{11} + 2c'_{12}\cos^2\theta\sin^2\theta + c'_{44}\sin^2 2\theta$$

$$c_{13} = c'_{12}, \quad c_{33} = c'_{11}, \quad c_{44} = c'_{44}, \quad \varepsilon_{11} = \varepsilon'_{11} \tag{3}$$

$$e_{15} = e'_{14}\sin 2\theta, \quad e_{31} = 0.5e'_{14}\sin 2\theta$$

where θ is the cutting angle of piezoelectric cubic crystal.

By substituting Eq. (2) into Eq. (1) we can obtain the governing equations for piezoelectric cubic crystal as

$$c_{11}u_{1,11} + c_{44}u_{1,33} + \left(c_{13} + c_{44}\right)u_{3,13} + \left(e_{15} + e_{31}\right)\varphi_{,13} = \rho\ddot{u}_1$$

$$\left(c_{13} + c_{44}\right)u_{1,13} + c_{33}u_{3,33} + c_{44}u_{3,11} + e_{15}\varphi_{,11} = \rho\ddot{u}_3 \tag{4}$$

$$\left(e_{15} + e_{31}\right)u_{1,13} + e_{15}u_{3,11} - \varepsilon_{11}\left(\varphi_{,11} + \varphi_{,33}\right) = 0$$

Considering a dielectric substrate occupying $0 > x_3 > -\infty$, the mechanical displacement and electric potential must satisfy the equation of motion and Laplace's equation according to the general theory of elasticity. Let $\bar{u}_1$, $\bar{u}_3$ and $\bar{\varphi}$ denote the mechanical displacement and electric potential in the dielectric substrate, then the governing equations for dielectric media can be obtained as

$$\bar{c}_{11}\bar{u}_{1,11} + \bar{c}_{44}\bar{u}_{1,33} + \left(\bar{c}_{13} + \bar{c}_{44}\right)\bar{u}_{3,13} = \bar{\rho}\ddot{\bar{u}}_1$$

$$\left(\bar{c}_{13} + \bar{c}_{44}\right)\bar{u}_{1,13} + \bar{c}_{11}\bar{u}_{3,33} + \bar{c}_{44}\bar{u}_{3,11} = \bar{\rho}\ddot{\bar{u}}_3 \tag{5}$$

$$\bar{\varepsilon}_{11}\left(\bar{\varphi}_{,11} + \bar{\varphi}_{,33}\right) = 0$$

where $\bar{c}_{11}$, $\bar{c}_{13}$ and $\bar{c}_{44}$ are the elastic constant of dielectric media, $\bar{\varepsilon}_{11}$ and $\bar{\rho}$ are dielectric constant and mass density. A short line lying on the variables denotes the fields of dielectric substrate, hereafter.

On the top of the piezoelectric layer, the mechanical traction-free conditions are

$$\sigma_{13}\left(x_1, h\right) = 0, \quad \sigma_{33}\left(x_1, h\right) = 0 \tag{6}$$

At the same time, two kinds of electrical boundary conditions existing in practical applications are proposed to restraint the normal electric displacement or electric potential of the piezoelectric surface, i.e.

$$D_3(x_1, h) = 0 \qquad (7)$$

for electrically open case and

$$\varphi(x_1, h) = 0 \qquad (8)$$

for electrically shorted case.

For a piezoelectric layered system, the interface between two constituents is usually assumed to be a perfect bonding interface for simplification which means that all the fields including the mechanical displacement, the stress, the electric potential and the electric displacement are continuous across the interface. However, the interface is always imperfect in most practical applications due to the various causes as mentioned in the previous section. It should be pointed out that not only the mechanical imperfection but also the electrical imperfection may occur at the interface of piezoelectric layered system. Jumps in mechanical or electrical quantities, or both, can occur at the imperfect interface [Li, Wei and Guo (2016)]. Instead of usual interface continuity conditions, we here consider a kind of interface possessing the special property of the mechanically compliant and dielectrically weakly conducting. In this case, the stresses and electric displacement are assumed to be continuous and the mechanical displacements and electric potential are discontinuous, that is

$$\sigma_{13} = \bar{\sigma}_{13} = K_T (u_1 - \bar{u}_1)$$
$$\sigma_{33} = \bar{\sigma}_{33} = K_N (u_3 - \bar{u}_3) \qquad (9)$$
$$D_3 = \bar{D}_3 = K_\beta (\varphi - \bar{\varphi})$$

where K_T and K_N are the tangential and normal interface parameters describing the bonding strength of mechanical fields, respectively, while the parameter K_β corresponds to the electrical imperfection. From Eq. (9), it is clear that the interface should be considered as perfect bonding when all the three interfacial parameters take infinite values. On the contrary, the covering layer and the substrate will be divorced from each other as the mechanically interfacial parameters K_T and K_N decreasing to zero. Physically speaking, the interface can be considered as an insulated interface when the electrical parameter K_β equals to zero. In addition, the mechanical displacement and electric potential in the substrate tend to zero far from the interface along the negative x_3 direction, i.e.,

$$\bar{u}_1 \to 0, \quad \bar{u}_3 \to 0, \quad \bar{\varphi} \to 0. \quad \text{as } x_3 \to -\infty \qquad (10)$$

3 General solutions and dispersion relations

In this section, we search for the solutions of Rayleigh-type wave satisfying Eqs. (4) and (5) under the conditions (6)-(10). Based on the partial wave method [Cheng and Sun (1975)], the solution of Eq. (4) can be assumed as

$$u_1 = Ae^{bkx_3}\cos[k(x_1 - vt)]$$

$$u_3 = Be^{bkx_3}\sin[k(x_1 - vt)] \tag{11}$$

$$\varphi = Ce^{bkx_3}\sin[k(x_1 - vt)]$$

where k is the wavenumber, and v stands for the phase velocity of Rayleigh-type wave. A, B and C are unknown wave amplitudes, b is an undetermined parameter.

Substituting Eq. (11) into Eq. (4), we can obtain

$$\left(c_{44}b^2 - c_{11} + \rho v^2\right)A + \left(c_{13} + c_{44}\right)bB + \left(e_{15} + e_{31}\right)bC = 0$$

$$\left(c_{13} + c_{44}\right)bA + \left(c_{44} - c_{33}b^2 - \rho v^2\right)B + e_{15}C = 0 \tag{12}$$

$$\left(e_{15} + e_{31}\right)bA + e_{15}B + \varepsilon_{11}\left(b^2 - 1\right)C = 0$$

For the above system of equations, to obtain a nontrivial solution of the resulting system, the determinant of the coefficient matrix must vanish, i.e.,

$$\begin{vmatrix} c_{44}b^2 - c_{11} + \rho v^2 & \left(c_{13} + c_{44}\right)b & \left(e_{15} + e_{31}\right)b \\ \left(c_{13} + c_{44}\right)b & c_{44} - c_{33}b^2 - \rho v^2 & e_{15} \\ \left(e_{15} + e_{31}\right)b & e_{15} & \varepsilon_{11}\left(b^2 - 1\right) \end{vmatrix} = 0 \tag{13}$$

Eq. (13) is a six-order equation in b with the phase velocity v as an unknown parameter. So for a given value of v, there are six roots satisfying Eq. (13) which denoted by b_i (i=1-6). Substituting the six roots of b_j into the last two equations of (12), the amplitude ratios $B_i = \chi_i A_i$ and $C_i = \eta_i A_i$ can be obtained, where

$$\chi_i = \frac{\begin{vmatrix} -\left(c_{44}b_i^2 - c_{11} + \rho v^2\right) & \left(e_{15} + e_{31}\right)b_i \\ -\left(c_{13}b_i + c_{44}b_i\right) & e_{15} \end{vmatrix}}{\begin{vmatrix} \left(c_{13} + c_{44}\right)b_i & \left(e_{15} + e_{31}\right)b_i \\ c_{44} - c_{33}b_i^2 - \rho v^2 & e_{15} \end{vmatrix}},$$

$$\eta_i = \frac{\begin{vmatrix} \left(c_{13} + c_{44}\right)b_i & -\left(c_{44}b_i^2 - c_{11} + \rho v^2\right) \\ c_{44} - c_{33}b_i^2 - \rho v^2 & -\left(c_{13}b_i + c_{44}b_i\right) \end{vmatrix}}{\begin{vmatrix} \left(c_{13} + c_{44}\right)b_i & \left(e_{15} + e_{31}\right)b_i \\ c_{44} - c_{33}b_i^2 - \rho v^2 & e_{15} \end{vmatrix}}.$$

The complete solutions of piezoelectric crystal must contain all of the six roots of b, so the displacements and electric potential can be obtained as

$$u_1 = \sum_{i=1}^{6} A_i e^{b_i k x_3} \cos[k(x_1 - vt)]$$

$$u_3 = \sum_{i=1}^{6} \chi_i A_i e^{b_i k x_3} \sin[k(x_1 - vt)] \tag{14}$$

$$\varphi = \sum_{i=1}^{6} \eta_i A_i e^{b_i k x_3} \sin[k(x_1 - vt)]$$

By applying the constitutive relations, the stresses and electric displacement can be obtained as

$$\sigma_{13} = \sum_{i=1}^{6} \left(c_{44} b_i + c_{44} \chi_i + e_{15} \eta_i\right) k A_i e^{b_i k x_3} \cos[k(x_1 - vt)]$$

$$\sigma_{33} = \sum_{i=1}^{6} \left(c_{33} b_i \chi_i - c_{13}\right) k A_i e^{b_i k x_3} \sin[k(x_1 - vt)] \tag{15}$$

$$D_3 = \sum_{i=1}^{6} \left(-e_{31} - \varepsilon_{11} b_i \eta_i\right) k A_i e^{b_i k x_3} \sin[k(x_1 - vt)]$$

For the dielectric substrate, the solutions to Eq. (5) have the following formulations

$$\bar{u}_1 = \bar{A} e^{\bar{b} k x_3} \cos[k(x_1 - vt)]$$

$$\bar{u}_3 = \bar{B} e^{\bar{b} k x_3} \sin[k(x_1 - vt)] \tag{16}$$

$$\bar{\varphi} = \bar{C} e^{\bar{b}' k x_3} \sin[k(x_1 - vt)]$$

where $\bar{A}$, $\bar{B}$ and $\bar{C}$ are unknown wave amplitudes, $\bar{b}$ and $\bar{b}'$ are attenuation coefficients in the substrate to be determined.

Substituting Eq. (16) into Eq. (5), we can obtain

$$\left(\bar{c}_{44} \bar{b}^2 - \bar{c}_{11} + \bar{\rho} v^2\right)\bar{A} + \left(\bar{c}_{13} + \bar{c}_{44}\right)\bar{b}\bar{B} = 0$$
$$\left(\bar{c}_{13} + \bar{c}_{44}\right)\bar{b}\bar{A} + \left(\bar{c}_{44} - \bar{c}_{11}\bar{b}^2 - \bar{\rho} v^2\right)\bar{B} = 0 \tag{17}$$

$$\bar{\varepsilon}_{11}\left(\bar{b}'^2 - 1\right)\bar{C} = 0 \tag{18}$$

Eq. (18) corresponds to the electric potential wave propagating in the dielectric substrate and decouples with the mechanical fields governed by Eq. (17). Since $\bar{C} \neq 0$, the electric attenuation parameter $\bar{b}'$ can be solved form Eq. (18) as a pair of real roots with opposite signs, i.e., $\bar{b}' = \pm 1$. It means that the electric potential wave in the dielectric media decays away (for $\bar{b}' = 1$) or increases away (for $\bar{b}' = -1$) from the interface as x3 increases. Here, the positive root $\bar{b}' = 1$ should be retained since the electric potential in the substrate must decay with increasing depth. To obtain a nontrivial solution of Eq. (17), the determinant of the coefficient matrix must vanish, i.e.,

$$\begin{vmatrix} \bar{c}_{44}\bar{b}^2 - \bar{c}_{11} + \bar{\rho}v^2 & (\bar{c}_{13} + \bar{c}_{44})\bar{b} \\ (\bar{c}_{13} + \bar{c}_{44})\bar{b} & \bar{c}_{44} - \bar{c}_{11}\bar{b}^2 - \bar{\rho}v^2 \end{vmatrix} = 0 \tag{19}$$

For a given value of v, the above equation yields four roots for $\bar{b}$ in the substrate. The two positive values of $\bar{b}$ should be retained in consideration of decaying wave modes in the substrate, which are denoted by $\bar{b}_j$ $(j=7-8)$. Thus, the complete solutions of dielectric substrate can be obtained as

$$\bar{u}_1 = \sum_{j=7}^{8} \bar{A}_j e^{\bar{b}_j kx_3} \cos[k(x_1 - vt)]$$

$$\bar{u}_3 = \sum_{j=7}^{8} \bar{\chi}_j \bar{A}_j e^{\bar{b}_j kx_3} \sin[k(x_1 - vt)] \tag{20}$$

$$\bar{\varphi} = \bar{C}e^{kx_3} \sin[k(x_1 - vt)]$$

where $\bar{\chi}_j = \dfrac{\bar{c}_{11} - \bar{c}_{44}\bar{b}_j^2 - \bar{\rho}v^2}{(\bar{c}_{13} + \bar{c}_{44})\bar{b}_j}$.

The stresses and electric displacement can be produced by taking account of the general elastic constitutive relations, as follows

$$\bar{\sigma}_{13} = \sum_{j=7}^{8} \left(\bar{c}_{44}\bar{b}_j + \bar{c}_{44}\bar{\chi}_j \right) k\bar{A}_j e^{\bar{b}_j kx_3} \cos[k(x_1 - vt)]$$

$$\bar{\sigma}_{33} = \sum_{j=7}^{8} \left(\bar{c}_{11}\bar{b}_j\bar{\chi}_j - \bar{c}_{13} \right) k\bar{A}_j e^{\bar{b}_j kx_3} \sin[k(x_1 - vt)] \tag{21}$$

$$\bar{D}_3 = -\bar{\varepsilon}_{11} k\bar{C}e^{kx_3} \sin[k(x_1 - vt)]$$

So far, the solutions for rotated cubic piezoelectricity and dielectric substrate are completely obtained. By taking advantage of the electro-mechanical conditions of the surface as well as the interfacial imperfection, a set of nine-order liner homogenous system with unknown constants A_n $(n=1\text{-}8)$ and $\bar{C}$ can be obtained as

$$[S]_{9\times9}\{X\} = 0 \tag{22}$$

where $\{X\} = \begin{bmatrix} A_n, & \bar{C} \end{bmatrix}^{\mathrm{T}}$, and the components of matrix *S* are listed in Appendix.

For the existence of a nontrivial solution of Eq. (22), if and only if the determinant of the coefficient matrix must vanish, and this leads to the dispersion relation as

$$\det(S) = 0 \tag{23}$$

4 Numerical results and discussions

In this section, numerical calculations are carried out to show the propagation characteristic of Rayleigh-type waves in piezoelectric layered systems of cubic crystals with electrically and mechanically interfacial imperfections. The piezoelectric cubic crystal is considered as Indium Arsenide (InAs) and the substrate is selected as Diamond. The material parameters of the InAs in the crystallographic coordinate system *XYZ* are [Auld (1973)]: $c'_{11} = 8.392$ (10^{10} N/m^2), $c'_{12} = 4.526$ (10^{10} N/m^2), $c'_{44} = 3.959$ (10^{10}N/m^2), $e'_{14} = -0.045$ (C/m^2), $\varepsilon'_{11} = 12.8$ (10^{-11} C^2/Nm^2), ρ=5700 (kg/m^3). The material parameters of the Diamond are [Benetti, Cannatà, Pietrantonio et al. (2005)]: $\overline{c}_{11}$=115.312 (10^{10} N/m^2), $\overline{c}_{13}$=8.644 (10^{10} N/m^2), $\overline{c}_{44}$=53.334 (10^{10} N/m^2), $\overline{\varepsilon}_{11}$=550 ($10^{-11}$ C^2/Nm^2), $\overline{\rho}$=3512 (kg/m^3). For convenience of calculation, three non-dimensional parameters are introduced to describe the interfacial imperfection, that is, $k_t = K_T h / c_{44}$, $k_n = K_N h / c_{44}$, $k_\beta = K_\beta h / \varepsilon_{11}$.

4.1 Effect of electrical boundary condition on dispersion curve

Dispersion curves of Rayleigh-type wave in InAs/Diamond layered structure under electrically open and shorted cases are respectively shown in Figs. 2(a) and 2(b), where θ=45° , $k_t = k_n = k_\beta$=5. It is found from Fig. 2 that phase velocity of the first mode starts from the Rayleigh wave velocity of Diamond (10937 m/s), monotonically decreases as the non-dimensional wavenumber increasing and tends towards the corresponding Rayleigh wave velocities of InAs (2237.34 m/s for electrically open circuit and 2237.29 m/s for electrically shorted circuit). The indistinct difference of the wave velocity at high frequency between the electrically open and shorted cases is because the piezoelectric constants of InAs are very small and the electro-mechanical coupling property is also weak. For the second mode and above, phase velocities uniformly start from the bulk shear wave velocity of Diamond (12322 m/s). These primary propagation characteristics of Rayleigh-type wave, e.g. the starting wave velocity at small wavenumber and the approaching wave velocity in the range of higher wavenumber, completely coincide with those given by Rose [Rose (1999)]. This coincidence can verify the validity of our analytical solution and numerical procedure. In view of the insignificant effect of electrical boundary conditions on dispersion curve and wave velocity, we thus focus on electrically open case in the following discussions.

4.2 Effect of cutting angle on phase velocity

Fig. 3 shows the effect of cut orientation on phase velocity of the first mode for selected values of non-dimensional wavenumbers. It is clear from Fig. 3 that phase velocity of Rayleigh-type wave is symmetric with respect to θ=45°. The wave velocity reaches the maximum value at θ=45° while minimum for the cases of θ=0° and 90°. This means that if we appropriately set the cut orientation of InAs crystal along the degree of 45° an optimal propagation behavior of Rayleigh-type wave can be achieved. For a SAW device, operating under a proper wave speed cannot only be an effective help for enhancing sensitivity, but also for the miniaturization of device.

4.3 Effect of interfacial imperfection on phase velocity

The effects of the tangential and normal interface parameters k_t and k_n on phase velocity of the first mode are illustrated in Fig. 4, where the cutting angle θ is selected as $45°$. It can be seen from Fig. 4 that both the tangential and normal imperfections consistently weaken the wave velocity of Rayleigh-type wave. Physically speaking, wave propagation is the propagation of mechanical energy. The interface has higher transmission capability of mechanical energy when it is mechanically perfect bonding. On the contrary, a mechanically imperfect bonding represents a deformable interface which has less stiffness comparing with a perfect interface. The degenerated interface can lead to the reduction of wave velocity. It is observed from Fig. 4 that the tangential interface parameter has smaller effect on wave velocity comparing with the normal imperfection. This is because the tangentially imperfect bonding only results in sliding contact, while the normal imperfection maybe leads to an extreme case of interfacial detachment and hence strongly affects the propagation behaviors of Rayleigh-type wave. It is also found that the interface can be regarded as a perfect bonding when the non-dimensional tangential parameter k_t is larger than about 20 and the normal parameter k_n about 40. On the other hand, the mechanical imperfection has great effects on phase velocity at relative small wavenumbers. But for higher frequency or large wavenumber, e.g., $kh>3$, the influence of mechanical imperfection on phase velocity gradually decays and thus the distinction between normal and tangential parameters turns to disappearance.

Fig. 5 shows the effect of the electrical interface parameters k_β on phase velocity, where $\theta=45°$. It can be seen from Fig. 5 that the electrical imperfection has very less effect on phase velocity comparing with the mechanical imperfection shown in Fig. 4. According to our calculation, the electrical imperfection makes a small reduction of wave velocity. When the non-dimensional imperfection parameter k_β decreases from 10 to zero, the decrease in phase velocity of Rayleigh-type wave is about within one decimal places. This is because the mechanical interaction at the interface of piezoelectric layer and dielectric substrate plays a dominant role in the piezoelectric coupling system during the propagation of Rayleigh-type waves. Under this special consideration and for the InAs/Diamond layered system, we can ignore the effect of electrical imperfection on wave velocity and thus focus on the mechanical imperfection in the design and application of InAs-based acoustic wave device.

5 Conclusions

Propagation of Rayleigh-type waves in layered structures consisting of a rotated piezoelectric cubic crystal imperfectly bonding onto a dielectric substrate is investigated in this paper. The imperfect interface is assumed as mechanically compliant and dielectrically weakly conducting condition. The exact dispersion relations for electrically open and shorted boundary conditions are derived in closed form. The numerical results show that: 1) the phase velocity is symmetric with respect to the cutting angle of 45° and can achieve the maximum propagation speed; 2) the electrical boundary conditions applied on the surface of the layered system have less effect on dispersion curves; 3) the mechanical imperfection can significantly affect the dispersion curves and then lowers the phase velocity because the deformable interface makes the interfacial stiffness

weaken. Further, the phase velocity is more sensitive to the normal imperfection comparing with that of tangential; 4) the electrical imperfection makes a relatively small reduction of phase velocity of Rayleigh-type wave comparing with the mechanical imperfection. These results can offer some fundamentals for understanding of piezoelectric semiconductor as well as the basis for design and application of piezoelectric SAW devices.
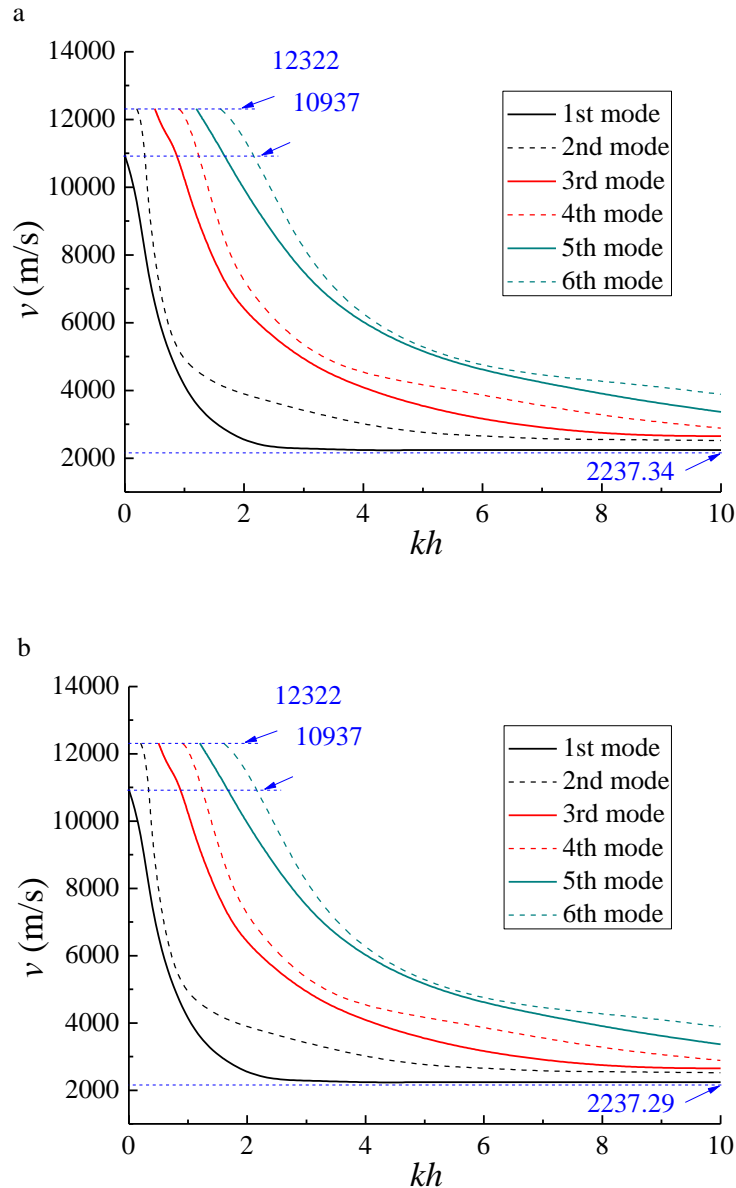

Figure 2: Dispersion curves of Rayleigh-type wave in InAs/diamond layered structure, where θ=45°, k_t=k_n=k_β=5. (a) electrically open case, (b) electrically shorted case
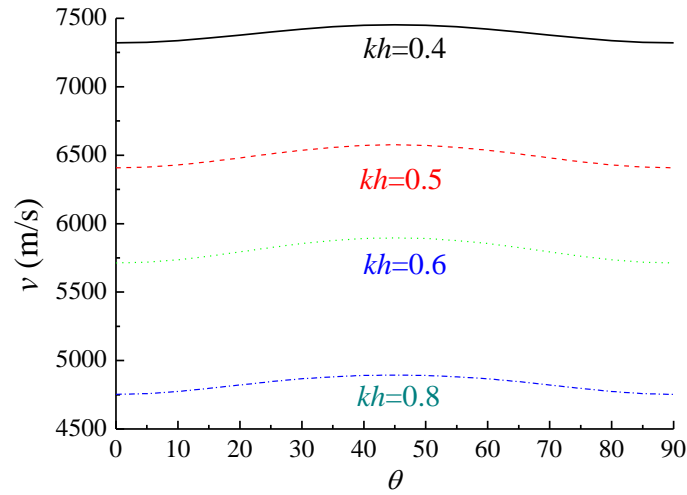
Figure 3: Effects of the cut orientation on phase velocity, where $k_t=k_n=k_\beta=5$
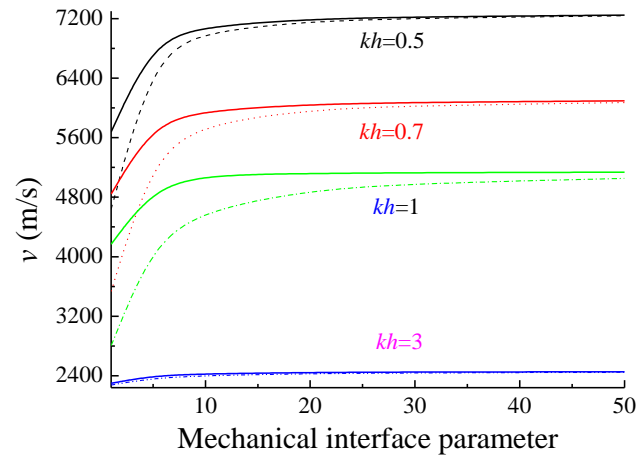

Figure 4: Effects of the mechanical interface parameters k_t, k_n on phase velocity, where $\theta=45°$, k_t in solid line and k_n in dash line
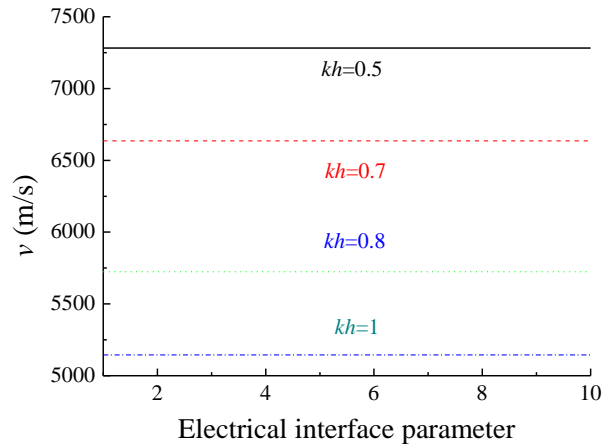
Figure 5: Effect of the electrical interface parameter k_β on phase velocity, where $\theta=45°$

References

Auld, B. A. (1973): *Acoustic Fields and Waves in Solids*. Wiley.

Benetti, M.; Cannatà, D.; Di Pietrantonio, F.; Fedosov, V. I.; Verona, E. (2005): Gigahertz-range electro-acoustic devices based on pseudo-surface-acoustic waves in AlN/diamond/Si structures. *Applied Physics Letters*, vol. 87, no. 3, 033504.

Bleustein, J. L. (1968): A new surface wave in piezoelectric materials. *Applied Physics Letters*, vol. 13, no. 12, pp. 412-413.

Bright, V. M.; Hunt, W. D. (1989): Bleustein-gulyaev waves in gallium arsenide and other piezoelectric cubic crystals. *Journal of Applied Physics*, vol. 66, no. 4, pp. 1556-1564.

Campbell, J. J.; Jones, W. R. (1968): A method for estimating optimal crystal cuts and propagation directions for excitation of piezoelectric surface waves. *IEEE Transactions on Sonics & Ultrasonics*, vol. 15, no. 4, pp. 209-217.

Chen, H.; Wang, J.; Du, J.; Yang, J. (2016): Propagation of shear-horizontal waves in piezoelectric plates of cubic crystals. *Archive of Applied Mechanics*, vol. 86, no. 3, pp. 517-528.

Chen, Z. G.; Hu, Y. T.; Yang, J. S. (2008): Shear horizontal piezoelectric waves in a piezoceramic plate imperfectly bonded to two piezoceramic half-spaces. *Journal of Mechanics*, vol. 24, no. 3, pp. 229-239.

Cheng, N. C.; Sun, C. T. (1975): Wave propagation in two-layered piezoelectric plates. *Journal of the Acoustical Society of America*, vol. 57, no. 3, pp. 632-638.

Curtis, R. G.; Redwood, M. (1973): Transverse surface waves on a piezoelectric material carrying a metal layer of finite thickness. *Journal of Applied Physics*, vol. 44, no. 5, pp. 2002-2007.

Fan, H.; Yang, J.; Xu, L. (2006): Piezoelectric waves near an imperfectly bonded interface between two half-spaces. *Applied Physics Letters*, vol. 88, no. 20, pp. 203509.

Fan, H.; Yang, J.; Xu, L. (2006): Antiplane piezoelectric surface waves over a ceramic half-space with an imperfectly bonded layer. *IEEE Transactions on Ultrasonics Ferroelectrics & Frequency Control*, vol. 53, no. 9, pp. 1695-1698.

Garner, H. R.; Ohkawa, T. (2002): High-frequency acoustic interaction of resonant systems using SAWs. *IEEE Transactions on Ultrasonics Ferroelectrics & Frequency Control*, vol. 40, no. 1, pp. 69-72.

Ghasemi, H.; Park, H. S.; Rabczuk, T. (2017): A level-set based IGA formulation for topology optimization of flexoelectric materials. *Computer Methods in Applied Mechanics and Engineering*, vol. 313, pp. 239-258.

Ghasemi, H.; Park, H. S.; Rabczuk, T. (2018): A multi-material level set-based topology optimization of flexoelectric composites. *Computer Methods in Applied Mechanics and Engineering*, vol. 332, pp. 47-62.

Gulyaev, Y. V. (1969): Electroacoustic surface waves in solids. *Soviet Journal of Experimental & Theoretical Physics Letters*, vol. 9, no. 1, pp. 37.

Hamdia, K. M.; Ghasemi, H.; Zhuang X.; Alajlan, N.; Rabczuk, T. (2018): Sensitivity and uncertainty analysis for flexoelectric nanostructures. *Computer Methods in Applied Mechanics and Engineering*, vol. 337, pp. 95-109.

Huang, Y.; Li, X. F. (2011): Interfacial waves in dissimilar piezoelectric cubic crystals with an imperfect bonding. *IEEE Transactions on Ultrasonics Ferroelectrics & Frequency Control*, vol. 58, no, 6, pp. 1261-1265.

Jakoby, B.; Vellekoop, M. J. (1997): Properties of Love waves: applications in sensors. *Smart Materials & Structures*, vol. 6, no. 6, pp. 668-679.

Lavrentyev, A. I, Rokhlin, S. I. (1998): Ultrasonic spectroscopy of imperfect contact interfaces between a layer and two solids. *Journal of the Acoustical Society of America*, vol. 103, pp. 657-664.

Lewis, M. F. (1995): Rayleigh waves-a progress report. *European Journal of Physics*, vol. 16, no. 1, pp. 1-7.

Li, L.; Wei, P. J.; Guo, X. (2016): Rayleigh wave on the half-space with a gradient piezoelectric layer and imperfect interface. *Applied Mathematical Modelling*, vol. 40, no. 19-20, pp. 8326-8337.

Li, P.; Jin, F. (2012): Bleustein-Gulyaev waves in a transversely isotropic piezoelectric layered structure with an imperfectly bonded interface. *Smart Materials & Structures*, vol. 21, no. 4, pp. 45009-45017.

Li, Y. D.; Lee, K. Y. (2010): Effect of an imperfect interface on the SH wave propagating

in a cylindrical piezoelectric sensor. *Ultrasonics*, vol. 50, no. 4-5, pp. 473-478.

Liu, J.; Wang, Y.; Wang, B. (2010): Propagation of shear horizontal surface waves in a layered piezoelectric half-space with an imperfect interface. *IEEE Transactions on Ultrasonics Ferroelectrics & Frequency Control*, vol. 57, no. 8, pp. 1875-1879.

Ma, C. C.; Wu, W. C. (2009): Analytical full-field solutions of a piezoelectric layered half-plane subjected to generalized loadings. *Computers, Materials & Continua*, vol. 11, no. 2, pp. 79-107.

Morocha, A. K. (2010): On the theory of Love waves in heterostructures with hexagonal symmetry. Semiconductors, vol. 44, no. 13, pp. 1625-1630.

Nanthakumar, S. S.; Lahmer, T.; Zhuang, X.; Zi, G.; Rabczuk, T. (2016): Detection of material interfaces using a regularized level set method in piezoelectric structures. *Inverse Problems in Science and Engineering*, vol. 24, no. 1, pp. 153-176.

Nanthakumar, S. S.; Zhuang, X.; Park, H. S.; Rabczuk, T. (2017): Topology optimization of flexoelectric structures. *Journal of the Mechanics and Physics of Solids*, vol. 105, pp. 217-234.

Nguyen, B. H.; Nanthakumar, S. S.; Zhuang X.; Wriggers, P.; Jiang, X. et al. (2018): Dynamic flexoelectric effect on piezoelectric nanostructures. *European Journal of Mechanics-A/Solids*, vol. 71, pp. 404-409.

Nie, G. Q.; Liu, J. X.; Li, M. (2015): Effect of an initial stress on SH-type guided waves propagating in a piezoelectric layer bonded on a piezomagnetic substrate. *Computers, Materials & Continua*, vol. 48, no. 3, pp. 133-145.

Nie, G. Q.; Liu, J. X.; Liu, X. L. (2016): Lamb wave propagation in a piezoelectric/piezomagnetic bi-material plate with an imperfect interface. *Acta Acustica United with Acustica*, vol. 102, no. 5, pp. 893-901.

Qian, Z. H.; Jin, F.; Hirose, S. (2011): Dispersion characteristics of transverse surface waves in piezoelectric coupled solid media with hard metal interlayer. *Ultrasonics*, vol. 51, no. 8, pp. 853-856.

Qian, Z. H.; Hirose, S. (2012): Theoretical validation on the existence of two transverse surface waves in piezoelectric/elastic layered structures. *Ultrasonics*, vol. 52, no. 3, pp. 442-446.

Rio, J. C. G. D.; Velasco, V. R. (1985): Acoustic surface waves in piezoelectric cubic crystals. *Surface Science*, vol. 162, no. 1, pp. 138-143.

Rose, J. L. (1999): *Ultrasonic Waves in Solid Media*. Cambridge University Press.

Singh, A. K.; Chaki, M. S.; Hazra, B.; Mahto, S. (2017): Influence of imperfectly bonded piezoelectric layer with irregularity on propagation of Love-type wave in a reinforced composite structure. *Structural Engineering & Mechanics*, vol. 62, no. 3, pp. 325-344.

Singh, A. K.; Das, A.; Mistri, K. C.; Chattopadhyay, A. (2017): Green's function approach to study the propagation of SH-wave in piezoelectric layer influenced by a point source. *Mathematical Methods in the Applied Sciences*, vol. 40, no. 13, pp. 4771-4784.

Singh, A. K.; Kumar, S.; Chattopadhyay, A. (2015): Love-type wave propagation in a piezoelectric structure with irregularity. *International Journal of Engineering Science*, vol. 89, pp. 35-60.

Singh, A. K.; Kumar, S.; Kumari, R. (2018): Impact of interfacial imperfection on transverse wave in a functionally graded piezoelectric material structure with corrugated boundaries. *The European Physical Journal Plus*, vol. 133, no. 3, pp. 120-134.

Singh, A. K.; Parween, Z.; Kumar, S.; Chattopadhyay, A. (2018): Propagation characteristics of transverse surface wave in a heterogeneous layer cladded with a piezoelectric stratum and an isotropic substrate. *Journal of Intelligent Material Systems and Structures*, vol. 29, no. 4, pp. 636-652.

Sun, C. T.; Cheng, N. C. (1974): Piezoelectric waves on a layered cylinder. *Journal of Applied Physics*, vol. 45, no. 10, pp. 4288-4294.

Thai, T. Q.; Rabczuk, T.; Zhuang, X. (2018): A large deformation isogeometric approach for flexoelectricity and soft materials. *Computer Methods in Applied Mechanics and Engineering*, vol. 341, pp. 718-739.

Tseng, C. C. (1970): Piezoelectric surface waves in cubic crystals. *Journal of Applied Physics*, vol. 41, no. 6, pp. 2270-2276.

Vig, J. R.; Ballato, A. (1998): Comments on the effects of nonuniform mass loading on a quartz crystal microbalance. *IEEE Transactions on Ultrasonics Ferroelectrics & Frequency Control*, vol. 45, no. 5, pp. 1123-1124.

Xu, L. M.; Fan, H.; Chen, M.; Li, H. (2006): Modeling piezoelectric interfacial wave near an imperfect interface. *Journal of Electronic Science and Technology of China*, vol. 4, no. 3, pp. 269-273.

Zakharenko, A. A. (2005): Love-type waves in layered systems consisting of two cubic piezoelectric crystals. *Journal of Sound & Vibration*, vol. 285, no. 4-5, pp. 877-886.

Zakharenko, A. A. (2005): Dispersive Rayleigh type waves in layered systems consisting of piezoelectric crystals bismuth silicate and bismuth germanate. *Acta Acustica United with Acustica*, vol. 91, no. 4, pp. 708-715.

Zakharenko, A. A. (2010): New interfacial shear-horizontal waves in piezoelectric cubic crystals. *Journal of Electromagnetic Analysis & Applications*, vol. 2, no. 11, pp. 633-639.

Zhang, R.; Feng, W. J. (2012): SH surface waves in a dielectric layered piezoelectric half space loaded with a liquid layer. *Acta Acustica United with Acustica*, vol. 98, no. 3, pp. 378-383.

Appendix

The non-zero components of matrix *S* for electrically open case:

$$S(1,i) = k_t , \quad S(1,j) = -k_t - \overline{c}_{44}\overline{b}_j h / c_{44} - \overline{c}_{44}\overline{\chi}_j h / c_{44}, \quad S(2,i) = k_n \chi_i ,$$

$$S(2,j) = -k_n \overline{\chi}_j - \overline{c}_{11}\overline{b}_j \overline{\chi}_j h / c_{44} + \overline{c}_{13} h / c_{44}, \quad S(3,i) = k_\beta \eta_i, \quad S(3,j) = 0,$$

$S(3,9) = -k_\beta \eta_i + \bar{\varepsilon}_{11} h / \varepsilon_{11}$, $S(4,i) = -e_{31} - \varepsilon_{11} b_i \eta_i$, $S(4,j) = 0$, $S(4,9) = \bar{\varepsilon}_{11}$,

$S(5,i) = c_{44} b_i + c_{44} \chi_i + e_{15} \eta_i$, $S(5,j) = -\bar{c}_{44} \bar{b}_j - \bar{c}_{44} \bar{\chi}_j$, $S(6,i) = c_{33} b_i \chi_i - c_{13}$,

$S(6,j) = -\bar{c}_{11} \bar{b}_j \bar{\chi}_j + \bar{c}_{13}$, $S(7,i) = (c_{44} b_i + c_{44} \chi_i + e_{15} \eta_i) e^{b_i k h}$,

$S(8,i) = (c_{33} b_i \chi_i - c_{13}) e^{b_i k h}$, $S(9,i) = (-e_{31} - \varepsilon_{11} b_i \eta_i) e^{b_i k h}$, where i=1~6, j=7~8.

By replacing the $S(9,i)$ with $\eta_i e^{b_i k h}$ the dispersion relation for electrically shorted case can be obtained.